organics

MDPI

Article

1,5-Acrylodan: A Fluorescent Bioconjugate Sensor of Protic Environments

Jake Morrin, Matthew Petitt and Christopher Abelt *

Department of Chemistry, College of William and Mary, Williamsburg, VA 23185, USA; jtmorrin@wm.edu (J.M.); petittmj@odu.edu (M.P.)
* Correspondence: cjabel@wm.edu; Tel.: +1-(757)-221-2677

Abstract: 1,5-Acrylodan (1-(5-(dimethylamino)naphthalen-1-yl)prop-2-en-1-one) is prepared in six steps from 1-nitronaphthalene and 19% overall yield. The last three steps involve an aryllithium-directed nucleophilic addition, catalytic Kulinkovich cyclopropanation, and copper-catalyzed oxidative ring-opening to generate the acryloyl moiety. The fluorescent properties of 1,5-Acrylodan (AC) are reported. These include its solvatochromism and H-bond quenching by protic solvents. Its use as a bioconjugate sensor is demonstrated with Human Serum Albumin (HSA) through its covalent attachment to Human Serum Albumin (HSA) at the free cysteine-34 moiety. Unfolding studies with guanidinium chloride (GdmCl) and sodium dodecyl sulfate (SDS) are conducted to illustrate how the fluorophore responds to changes in both micropolarity and exposure to water.

Keywords: fluorescence; sensor; micropolarity; H-bond quenching

1. Introduction

One approach to the determination of biomolecular structure and dynamics is through the use of suitable probes. Common techniques include radioisotopic labeling, the addition of radioactive tracers, the addition of colorimetric biosensors, and the use of bioelectrochemical sensors for the determination of redox activity in reductive enzymes [1]. Fluorophoric chemical probes offer a facile means to derive accurate and precise structural information. Fluorescent tagging remains a foundational approach in the study of biochemical compounds. Fluorescent tagging is non-destructive, requires relatively low concentrations of the fluorescent species, and affords a broad array of probe properties and functionalities [2]. Moreover, fluorescent labeling can be accomplished in a site-selective manner. Organic fluorophores that develop a stable, covalent linkage with specific residues of the target biomolecule are preferred for labeling proteins. A variety of organic fluorophores have been designed for site-selective fluorescent labeling. With native proteins, selective fluorophore labeling proceeds through the fluorophore-residue reactions of serine/tyrosine/threonine, lysine, or cysteine—broadly known as hydroxyl, amine, and thiol labeling, respectively [2]. The sulfhydryl side-chain of cysteine is a common residue for the chemical attachment of organic fluorophores, largely as a consequence of the high nucleophilicity and low abundance of the unbridged thiol moiety in vivo [3]. Such characteristics permit site-selective functionalization of free cysteine residues by electrophilic fluorophores, often proceeding through a Michael/conjugate addition mechanism. Human serum albumin (HSA) is an ideal model protein to demonstrate selective functionalization (Figure 1). HSA serves as the primary determinant of plasma colloid osmotic pressure and acts as a critical modulator of fluid distribution across the human circulatory system [4]. While HSA contains many cysteine moieties, only the one at position 34 is not involved in a disulfide bond.

check for updates

Citation: Morrin, J.; Petitt, M.; Abelt, C. 1,5-Acrylodan: A Fluorescent Bioconjugate Sensor of Protic Environments. *Organics* **2024**, *5*, 493–506. https://doi.org/10.3390/org5040026

Academic Editor: Neal Hickey

Received: 27 September 2024
Revised: 22 October 2024
Accepted: 4 November 2024
Published: 7 November 2024

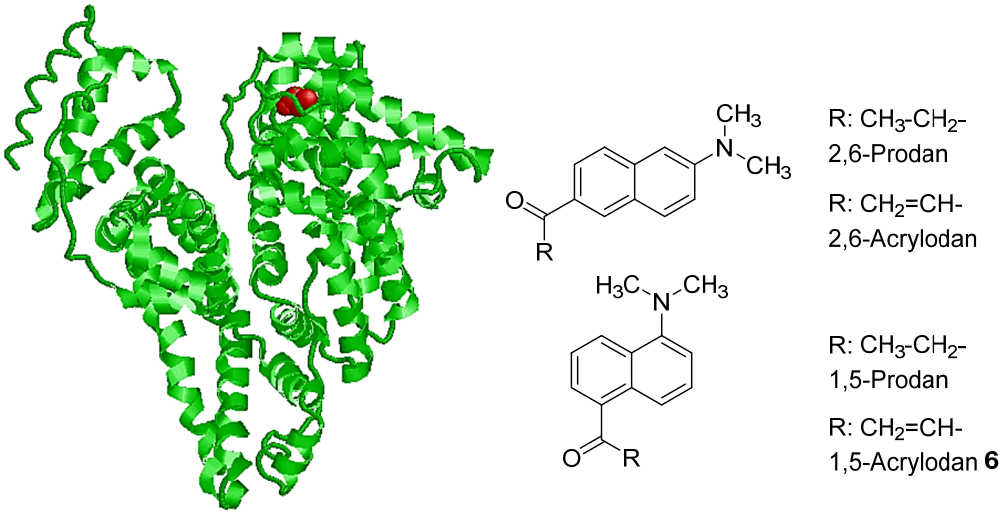

Figure 1. Human serum albumin (**left**, PDB: 1AO6, Cys-34 shown in red) and Prodan structures (**right**).

Small-molecule organic fluorophores share a common set of structural and electronic characteristics. As a general rule, these fluorophores have a rigid, π-conjugated aromatic scaffold with attached functional groups. Fluorescent dyes such as BODIPY, Rhodamine, and Laurdan have seen significant use as chemical sensors for the determination of structure–activity relationships in biological systems [5,6]. The environment-dependent emission behaviors of such conjugated heteroatomic fluorophores can be engineered synthetically. A design in which electron-donating and electron-accepting heteroatomic moieties are attached across a conjugated fluorophore scaffold (a 'push-pull' fluorophore), for example, will provide variable fluorescence intensity depending on microenvironmental conditions (solvent exposure, environmental polarity, etc.) [6]. As such, the experiment-specific design of both the π-conjugated scaffold and the functional group adornment is fundamental to the extraction of biophysical information from fluorescence data. A well-known example of such utility is 6-propionyl-2-dimethylamino-naphthalene (2,6-Prodan, Figure 1). This small-molecule organic fluorophore has been widely applied to the study of solvation dynamics in polar solutions [7,8].

The fluorescence properties of 2,6-Prodan rest upon the dual characteristic functionalities of the conjugated molecule: first, the dimethylamine moiety at the 2-naphthyl position, and second, the propionyl moiety at the 6-naphthyl position. The former permits charge transfer to the latter via the π naphthalene system upon photoexcitation. This charge transfer affects a substantial change in the excited-state molecular dipole moment and affords variable fluorescence characteristics that depend upon local environmental polarity. Consequently, 2,6-Prodan has seen significant adoption as a probe for microenvironmental polarity. The ubiquity of 2,6-Prodan has also encouraged its application to probe the molecular structure of biomolecules. For example, 2,6-Prodan noncovalently binds Human serum albumin (HSA) via a hydrophobic interaction with the warfarin binding site. This labelling is not durable and therefore not selective under dynamic conditions. This approach is inferior compared to a commensurate, covalently linked tag [9,10]. The principles of experimentally targeted fluorophore design, therefore, require more applicable fluorescent probes for the study of biomolecular dynamics.

Recent research has indicated that both 2,6-Prodan and 1,5-Prodan—a regioisomer of 2,6-Prodan—derive their fluorescence properties in polar solvents from a planar intramolecular charge transfer (PICT) excited state [11,12]. Photoexcitation of the Prodan derivative results in the net transfer of electron density from the dimethylamino moiety to the carbonyl moiety, thereby increasing the dipole moment of the molecule by nearly a factor of two [11]. The charge transfer gives rise to positive solvatochromism or a red shift in polar solvents. The emission from excited state structures where the dimethylamino group is

twisted (N-TICT) or where the propionyl group (O-TICT) is twisted is not supported by the behavior of model compounds. Forced-planar N-cyclized or propionyl-cyclized Prodan derivatives show similar fluorescence properties to the unconstrained parent structures [11]. The fluorescence of 2,6-Prodan and 1,5-Prodan are sensitive to solvent polarity, and thus they have been used as exogenous probes in the determination of biomolecular unfolding and hydration dynamics. While both 2,6 and 1,5-Prodan show similar solvatochromism, only 1,5-Prodan exhibits strong fluorescence quenching in alcohol solvents. The hydrogen-bonding interactions between the carbonyl moiety and the protic solvent in 1,5-Prodan lead to facile non-radiative deactivation, likely related to the slight carbonyl twisting due to the interaction with the peri-H [13]. Such quenching properties can be leveraged as a sensor of solvent polarity, and thus permit the further exploration of protein structure and dynamics.

A derivative of 2,6-Prodan, 6-acryloyl-2-dimethylaminonaphthalene (2,6-Acrylodan, or 2,6-AC, Figure 1), is a small-molecule organic naphthalene derivative with unique fluorophobic properties. First synthesized in 1983 by Prendergast et al., 2,6-AC is characterized by a dimethylamine moiety at the 2-naphthyl position and an α,β-unsaturated acryloyl moiety at the 6-naphthyl position [14]. 2,6-Acrylodan retains much of the saturated fluorophore's solvent sensitivity. Although 2,6-Acrylodan exhibits a lower fluorescence quantum yield than the saturated species, it behaves similarly with regard to its large-Stokes-shift positive solvatochromism [14,15]. The α,β-unsaturated acryloyl moiety of 2,6-Acrylodan allows for the conjugate addition of thiol nucleophiles, affecting a covalent thioester attachment and a significantly higher fluorescence quantum yield [14]. Thus, 2,6-Acrylodan retains the solvent-sensitivity advantages of 2,6-Prodan, while also permitting the facile, durable tagging of biomolecular species of interest.

The utility of 2,6-Acrylodan has been exploited in many biomolecular studies [16–23]. With HSA, 2,6-Acrylodan reacts to form a thioether linkage at Cys-34 in a manner that is both site-selective and singular. Analysis of fluorescence of 2,6-AC-HSA affords structural and protein-dynamic information. For the unfolding of HSA by guanidinium hydrochloride, the fluorescence intensity of 2,6-AC-HSA increases by ~15% between 0.0 and 2.0 M denaturant, followed by a linear decrease and an emissive red shift between 2.0 and 4.0 M. These data supported a distinct bipartite, multistep unfolding dynamic in the chemical denaturation of HSA, wherein Domain II unfolds before the AC-bound Domain I [24]. This conclusion contradicted prior research in support of concerted unfolding dynamics [25].

This paper details the total synthesis and fluorescence characteristics of 1,5-Acrylodan. Its use as a thiol-active fluorescent tag is demonstrated with HSA. Its utility as a molecular probe is shown through protein unfolding with sodium dodecyl sulfate (SDS) and guanidinium hydrochloride (GdmCl).

2. Materials and Methods

All reactions were carried out in flame-dried glassware under an air atmosphere unless otherwise specified. Reaction mixtures were stirred under magnetic stirring and heated using an oil bath attached to a variable transformer. Air-free or moisture-sensitive reactions were carried out under an argon atmosphere. All commercially available chemicals and solvents were used as purchased or purified by standard procedures as noted. NMR spectra were obtained on a 400 MHz (^{1}H) and 100 MHz (^{13}C) Agilent 400 MHz spectrometer (Santa Clara, CA, USA). High-resolution ESI-MS was acquired with a Bruker Apex-Qe instrument (Bremen, Germany). Fluorescence measurements were taken on an Ocean Optics Maya 2000 Pro spectrophotometer (Orlando, FL, USA) with a 1 cm cuvette. Absorption spectroscopy used a miniature deuterium/tungsten lamp and emission spectroscopy used a 365 nm LED light source. Emission intensities were processed by subtracting the electronic noise, converting wavelengths to wavenumbers, multiplying by $\lambda^2/{\lambda_{max}}^2$ to account for the effect of the abscissa scale transformation [26], and dividing by the spectral response of the Hamamatsu S10420 CCD (Bridgewater, USA). Relative quantum yields were determined using anthracene as the reference (Φ = 0.30).

2.1. Preparation of 1,5-Acrylodan

2.1.1. 1-Bromo-5-nitronaphthalene (**1**)

Under magnetic stirring, 1-nitronapthalene (10 g, 57.7 mmol) was combined with iron (III) chloride hexahydrate (66.5 mg, 0.246 mmol), and the reaction mixture was heated to 90 °C in an oil bath and stirred until fully liquified. Afterward, bromine (3 mL, 58.2 mmol) was added dropwise to the reaction mixture under an ice-water-cooled condenser. Heating was continued for 1.5 h, and then the reaction was removed from the heat and allowed to cool to room temperature. The ensuing solid black-brown product was crushed, dissolved in 200 mL EtOH, and heated to boiling until all of the solids were dissolved. The solution was allowed to cool slowly over 6 h. The resultant crystals were isolated via vacuum filtration, washed with chilled ethanol (10 mL), and dried under a vacuum, affording compound **1** as yellow-orange needles (9.51 g, 37.7 mmol) in 65% yield. ^{1}H NMR (400 MHz, $CDCl_3$) δ = 8.62 (d, *J* = 8.7 Hz, 1H), 8.48 (d, *J* = 8.7 Hz, 1H), 8.24 (d, *J* = 7.5 Hz, 1H), 7.94 (d, *J* = 7.5 Hz, 1H), 7.67 (t, *J* = 8.1, 1H), 7.55 (t, *J* = 8.1, 1H); ^{13}C {1H} NMR (100 MHz, $CDCl_3$) δ = 147.0, 133.4, 132.6, 131.6, 129.4, 126.3, 125.5, 124.3, 123.5, 122.8.

2.1.2. 5-Bromonaphthalen-1-amine (**2**)

The recrystallized bromonitronaphthalene (**1**) above (9.51 g, 37.7 mmol) was dissolved in ethanol (160 mL) and placed under magnetic stirring at 0 °C. The solution was allowed to cool to temperature, after which tin powder (40.73 g, 0.343 mol) was added batchwise. Afterward, aq. HCl (82 mL, 0.492 mol, 6 M) was added dropwise, under vigorous stirring. The reaction mixture was allowed to stir for 10 h, and the temperature was permitted to rise to 20 °C. Following reaction completion, as monitored by TLC, the solution was transferred to an oil bath, heated to 70 °C, and allowed to stir until the grey-yellow reaction mixture became translucent. The solution was then vacuum-filtered to remove excess and insoluble tin; the resulting filtrate was cooled to room temperature, evaporated in vacuo, and dried under a vacuum (0.5 torr) for 2 h. Afterward, the resultant white-grey powder was dried over K_2CO_3, sonicated, and transferred into a Soxhlet extractor. The Soxhlet extraction was then charged with 300 mL of CH_2Cl_2 and allowed to run for 36 h. The organic filtrate was washed with H_2O (4 × 200 mL) after extraction. The ensuing aqueous fractions were combined, basified to pH ~12 (3.0 g NaOH), and extracted with CH_2Cl_2 (2 × 50 mL). All resultant organic fractions were combined, washed with sat. aq. NaCl (1 × 200 mL), dried over Na_2SO_4, and concentrated in vacuo. The amine product **2** (7.96 g, 35.8 mmol, 95% yield), a beige crystalline solid, was used without further purification. ^{1}H NMR (400 MHz, $CDCl_3$) δ = 7.54 (m, 2H), 7.47 (d, *J* = 8.5 Hz, 1H), 7.17 (t, *J* = 8.0 Hz, 1H), 6.98 (t, *J* = 8.0 Hz, 1H), 6.54 (d, *J* = 7.5 Hz, 1H), 3.83 (br. s, 2H); ^{13}C {1H} NMR (100 MHz, $CDCl_3$) δ = 142.5, 132.9, 130.1, 127.8, 124.9, 124.7, 123.6, 120.8, 118.0, 110.7.

2.1.3. 5-Bromo-*N*,*N*-dimethylnaphthalen-1-amine (**3**)

Bromoaminonaphthalene **2** (7.96 g, 35.8 mmol) was dissolved in DMF (20 mL) and treated with K_2CO_3 (12.37 g, 89.5 mmol) in an Ace-Thred pressure tube under magnetic stirring. After agitating for 10 min, methyl iodide (12.7 g, 89.5 mmol) was streamed into the solution. The tube was sealed and permitted to stir for 48 h. Afterward, the reaction mixture was decanted into acetone (50 mL) and vacuum-filtered. Precipitated solids were rinsed with acetone (10 mL); the ensuing filtrate was concentrated under reduced pressure, dissolved in petroleum ether (100 mL), and washed with H_2O (4 × 100 mL). The organic fraction was washed with sat. aq. NaCl (1 × 100 mL), dried over Na_2SO_4, and concentrated in vacuo. The resultant red-black oil was purified via vacuum distillation (65 °C, 0.5 torr) to afford the dimethylated product **4** (8.49 g, 33.9 mmol) as an orange-red oil in 95% yield. This product was used without further purification. ^{1}H NMR (400 MHz, $CDCl_3$) δ = 8.22 (d, *J* = 7.8 Hz, 1H), 7.84 (d, *J* = 7.9 Hz, 1H), 7.74 (d, *J* = 7.3 Hz, 1H), 7.46 (t, *J* = 7.8 Hz, 1H), 7.27 (t, *J* = 7.9 Hz, 1H), 7.08 (d, *J* = 7.3 Hz, 1H), 2.84 (s, 6H); ^{13}C {1H} NMR (100 MHz, $CDCl_3$) δ = 151.3, 133.3, 130.3, 130.0, 127.2, 125.3, 124.3, 123.2, 121.9, 114.9, 45.4.

2.1.4. Ethyl 5-(Dimethylamino)-1-naphthoate (**4**)

5-Bromo-*N*,*N*-dimethylnaphthalen-1-amine **3** (2.0 g, 8.00 mmol) was dissolved in dry THF (16 mL) and cooled to −78 °C under Ar. *N*-Butyllithium (3.5 mL, 8.8 mmol, 2.5 M in hexanes) was added dropwise over 15 min with stirring. After this addition, stirring was continued for 10 min., whereupon ethyl chloroformate (1.6 mL, 16.8 mmol) was added dropwise over 20 min. The reaction mixture was stirred at −78 °C for 2 h. The reaction was quenched with sat. aq. NH_4Cl (4 mL) and allowed to warm to room temperature. The mixture was diluted with H_2O (100 mL) and extracted with EtOAc/hexanes (1:1; 2 × 150 mL). The combined organic layers were washed with H_2O (100 mL) and sat. aq. NaCl (100 mL), dried over Na_2SO_4, and concentrated in vacuo. The ester (1.84 g, 7.55 mmol, 94% yield), a fluorescent green-yellow oil, was used without further purification. ^{1}H NMR (400 MHz, $CDCl_3$) δ = 8.50 (dd, *J* = 8.3, 7.7 Hz, 2H), 8.11 (d, *J* = 7.2 Hz, 1H), 7.49 (m, 2H), 7.14 (d, *J* = 7.2 Hz, 1H), 4.47 (q, *J* = 7.2 Hz, 2H), 2.88 (s, 6H), 1.45 (t, *J* = 7.2 Hz, 3H); ^{13}C {1H} NMR (100 MHz, $CDCl_3$) δ = 168.00, 151.24, 132.62, 129.68, 129.05, 128.12, 127.49, 125.71, 123.72, 120.54, 114.50, 61.03, 45.44, 14.40.

2.1.5. 1-(5-(Dimethylamino)naphthalen-1-yl)cyclopropan-1-ol (**5**)

Ethyl 5-(dimethylamino)-1-naphthoate **4** (1.00 g, 4.11 mmol) was dissolved in dry THF (17.5 mL) and cooled to 0 °C under Ar. Titatium (IV) isopropoxide (1.73 mL, 5.84 mmol) was added quickly and the reaction mixture was stirred for 15 min. Ethyl magnesium chloride (7.5 mL, 20 mmol, 2.7 M) was added dropwise over 1 h via a syringe pump. The reaction was stirred for 8 h during which the temperature rose to 20 °C. The reaction was quenched with sat. aq. NH_4Cl (5 mL) and filtered with suction. The resulting precipitate was dissolved in EtOAc (20 mL), sonicated, and filtered with suction. All filtrates were combined, diluted with H_2O (50 mL), and extracted with EtOAc (3 × 50 mL). The organic layers were combined, washed with H_2O (50 mL) and sat. aq. NaCl (50 mL), dried over Na_2SO_4, and concentrated in vacuo. The cyclopropanol product (0.384 g, 1.69 mmol, 41% yield by NMR), a yellow-brown oil, was not fully separable from a co-eluting byproduct. It was used without further purification. ^{1}H NMR (400 MHz, $CDCl_3$) δ = 8.24 (m, 2H), 7.50 (m, 2H), 7.31 (dd, *J* = 8.3, 7.4 Hz, 1H), 7.12 (d, *J* = 7.4 Hz, 1H), 2.88 (s, 6H), 1.32 (m, 1H), 1.06 (m, 1H); ^{13}C {1H} NMR (100 MHz, $CDCl_3$) δ = 151.70, 138.31, 133.87, 129.68, 126.39, 125.91, 125.15, 124.59, 120.22, 114.35, 57.34, 45.57.

2.1.6. 1-(5-(Dimethylamino)naphthalen-1-yl)prop-2-en-1-one (**6**)

Cyclopropanol **5** (0.384 g, 1.69 mmol) was dissolved in methanol (5.5 mL) and treated with $Cu(OAc)_2$ (62 mg, 0.34 mmol) under air. The reaction was stirred for 30 min at room temperature. Next, the reaction mixture was concentrated in vacuo, dissolved in EtOAc (25 mL), and decanted into H_2O (50 mL). The aqueous layer was extracted with EtOAc (3 × 20 mL); all organic fractions were combined, washed with H_2O (25 mL) and sat. aq. NaCl (25 mL), dried over Na_2SO_4, and concentrated in vacuo. The residue was purified through column chromatography on silica gel with gradient elution (0 → 30% EtOAc in hexanes), affording the title compound **6** (0.320 g, 1.42 mmol) as a fluorescent yellow oil in 84% yield (19% from nitronaphthalene). ^{1}H NMR (400 MHz, $CDCl_3$) δ = 8.43 (d, *J* = 8.6 Hz, 1H), 7.91 (d, *J* = 8.6 Hz, 1H), 7.66 (d, *J* = 7.1 Hz, 1H), 7.52–7.43 (m, 2H), 7.13 (d, *J* = 7.6 Hz, 1H), 6.92 (dd, *J* = 10.6, 17.4 Hz, 1H), 6.24 (d, *J* = 17.4 Hz, 1H), 6.04 (d, *J* = 10.6 Hz, 1H), 2.89 (s, 6H); ^{13}C {1H} NMR (100 MHz, $CDCl_3$) δ = 196.51, 151.29, 137.19, 136.35, 131.84, 131.41, 129.38, 127.93, 127.37, 127.36, 123.56, 120.27, 114.69, 45.36.

HRMS (ESI): calcd. for $C_{15}H_{15}NONa^+$ $[M + Na]^+$ 248.10459; found 248.10443.

2.2. 1,5-Acrylodan-Human Serum Albumin Conjugate (1,5-AC-HSA)

1,5-Acrylodan-labelled HSA (1,5-AC-HSA) was prepared using the method of Wang et al. with minor modifications [27]. Purified **6** (6.0 mg, 0.027 mmol) was dissolved in acetonitrile (1 mL) and streamed into a solution of fatty-acid-free human serum albumin (1.592 g, 0.024 mmol) in aqueous sodium phosphate buffer (pH = 7.0 ± 0.5) under magnetic

stirring. The aqueous reaction mixture was covered with plastic wrap and allowed to stir, gently, for 10 h at 20 °C. Following reaction completion, the aqueous 1,5-Ac-HSA solution was loaded into dialysis sacks (MWCO 12,000 Da; Millipore-Sigma, Burlington, VT, USA) and dialyzed against an initial 1 L of 5% acetonitrile in the buffer. The buffer solution was changed four times after intervals of 8 h. The dialyzed solution was passed down a Sephadex G-25 size-exclusion column, then covered with plastic wrap and stored at 6 °C until use. The concentration of the above sample was determined to be 50 µM by its absorption at 308 nm assuming it has the same molar absorptivity as **6**.

Denaturation samples with guanidine hydrochloride were prepared using the method of Kamal et al. with minor modifications [28]. The above 1,5-Ac-HSA solution (200 µL ea.) was added to a series of nine 5 mL volumetric flasks. Variable amounts of aqueous guanidine hydrochloride (GdmHCl) were added to each to give final concentrations ranging from 0–8 M after dilution with buffer. Samples were agitated to promote equilibration, then allowed to stand and denature for 2 h. The solutions were re-agitated before measuring their emission.

Denaturation samples with sodium dodecyl sulfate (SDS) were prepared with a 1,5-Ac-HSA solution (200 µL ea.) and buffer (800 µL ea.). Variable aliquots of 2.1 mM SDS were added (0 → 50 µL) and the solutions were agitated and allowed to stand overnight before measuring their emission. The emission intensity was adjusted to account for the slight dilution.

3. Results

*3.1. Synthesis of 1,5-Acrylodan (**6**)*

1,5-Acrylodan (**6**) was prepared in six steps and 19% overall yield starting with 1-nitronaphthalene (Scheme 1). The synthesis of the methyl ester derivative of **4** has been reported [29]. In the current method, the ethyl ester is generated by reacting the naphthyl lithium intermediate with ethyl chloroformate in 95% yield. The reported route quenches the Grignard reagent derived from **3** with CO_2 and subsequently esterifies the resulting carboxylic acid. The naphthyl lithium intermediate derived from **3** has a high propensity for H-atom abstraction and gave poor conversions with electrophiles bearing acidic hydrogens, especially those adjacent to a carbonyl. The ethyl ester **4** is remarkably resistant to nucleophilic attack, e.g., with hydroxide, Grignard, and alkyl lithium reagents. However, the Kulinkovich reaction proved moderately successful (41%) with **4**. In this method, the ester is treated with two equivalents of ethyl Grignard in the presence of $Ti(OiPr)_4$ to afford the cyclopropanol product [30]. We found that three equivalents of ethyl Grignard gave the best yields, but that significant unidentified impurities always accompanied the reaction. The desired acryloyl moiety results from oxidative ring-opening with $Cu(OAc)_2$. The Kulinkovich reaction avoids the use of nucleophilic vinyl reagents with the ester.

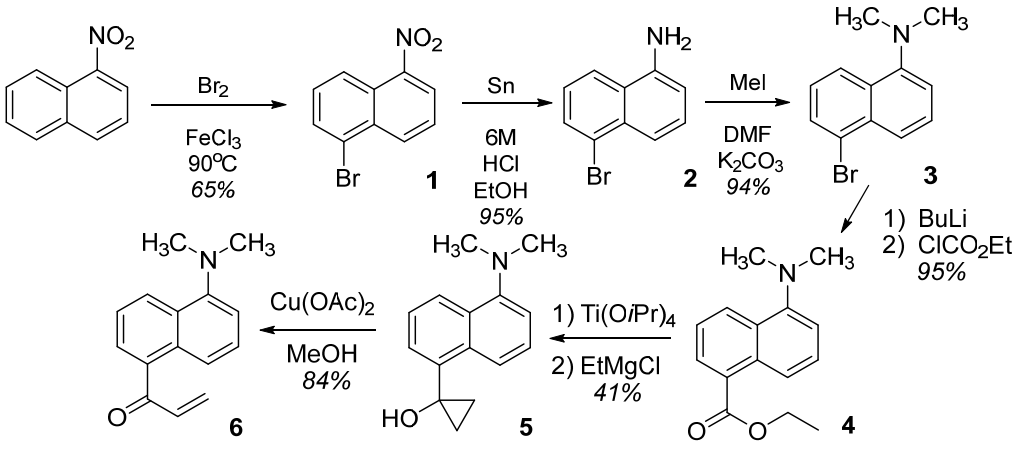

Scheme 1. Synthetic route to 1,5-Acrylodan (**6**).

3.2. Photophysical Characterization of 1,5-Acrylodan

3.2.1. Absorption Spectroscopy

The absorption spectrum of **6** in ethanol shows a broad shoulder centered at 308 nm (Figure 2). The shoulder extends from 294 nm to 315 nm over which the absorbance is nearly the same. At 365 nm, the fluorescence excitation wavelength, the absorbance is 43% of that at 308 nm.

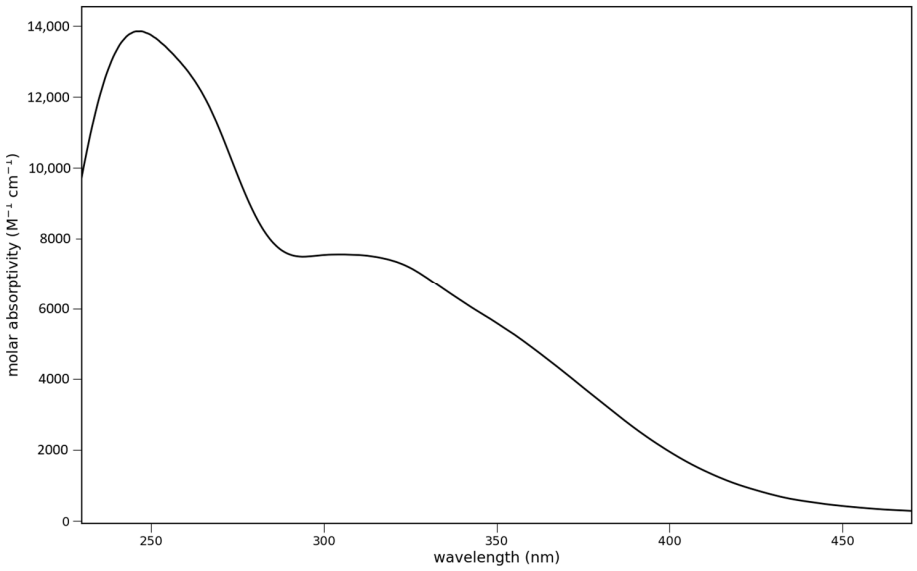

Figure 2. Absorption spectrum of **6** in ethanol (1.1×10^{-4} M).

3.2.2. Fluorescence Spectroscopy

The relative fluorescence quantum yield for **6** in toluene was determined using anthracene as a reference (Φ = 0.30). This fluorophore shows strong solvatochromism (*vide infra*) and gives the strongest emission in toluene. The relative quantum yield is 0.26 ± 0.03.

Solvatochromism studies showed that the fluorescence maximum of **6** varies with the polarity of the solvent. The maximum, expressed in wavenumbers, decreases with increasing solvent polarity. This trend is typical for Prodan and derivatives and is consistent with an intramolecular charge-transfer excited state. Polar solvents are better able to stabilize the greater charge separation in the excited state resulting in lower energy emission. The fluorescence in solvents ranging from apolar and aprotic to polar and protic is shown below (Figure 3).

Solvatochromism can be exhibited by a plot of the emission maximum vs. some measure of the solvent polarity. One commonly used polarity parameter is Reichardt's $E_T(30)$ value [31]. A plot of the emission maxima vs. the $E_T(30)$ parameter is shown in Figure 4. The magnitude of the slope is a measure of how strongly the solvent stabilizes the excited state. The slope of -137 indicates a reasonably strong stabilizing effect. The emission maxima range over 2000 cm^{-1} from toluene (apolar, aprotic) to isopropanol (polar, protic). Points for cyclohexane, ethanol, and methanol are not shown. The emission for cyclohexane is typically at much higher energy (here, 18,500 cm^{-1}) due to incomplete ICT. The emission maxima for ethanol and methanol are unreliable because the quenching is so strong.

Solvatochromism studies show that the fluorescence intensity of **6** not only varies with solvent polarity but also with proticity. While the fluorescence is weaker in cyclohexane than in toluene, it otherwise decreases monotonically with increasing polarity. In cyclohexane, the weaker emission has been ascribed to faster intersystem crossing to a triplet state. The weaker emission in successively polar solvents has been ascribed to the energy-gap law where non-radiative deactivation is faster as the energy gap between the excited state and the ground state decreases [11].

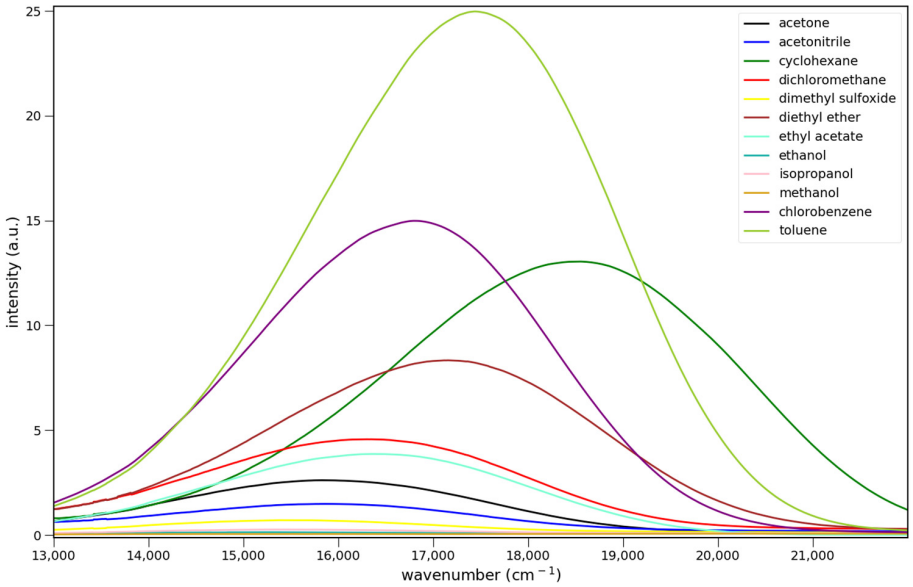

Figure 3. Fluorescence spectra of 1.3×10^{-5} M **6** in various solvents. Excitation at 365 nm.

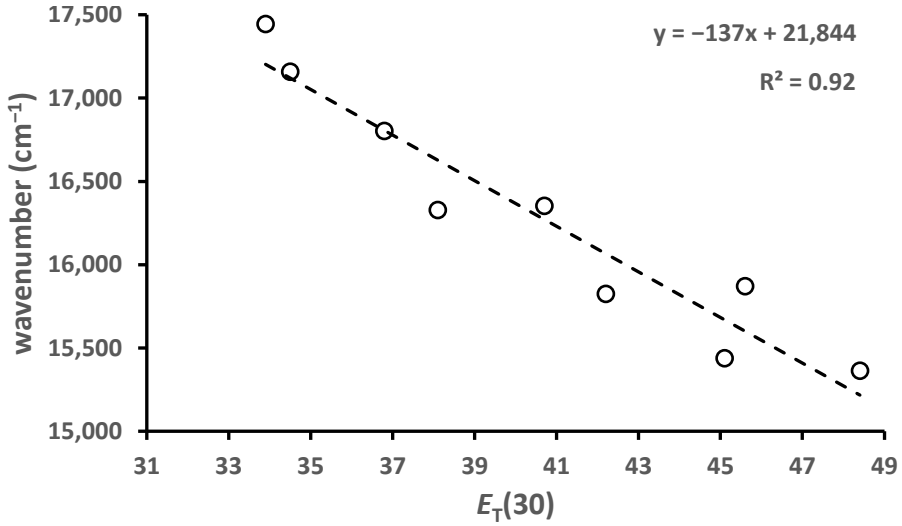

Figure 4. Plot of the fluorescence emission maxima vs. $E_T(30)$ for the spectra and solvents in Figure 3 and best-fit line. Points for cyclohexane, ethanol, and methanol are not shown.

Alcohols strongly quench the fluorescence, much more so than aprotic solvents, like acetonitrile, with equal polarity. The fluorescence spectra of **6** in a range of protic solvents are shown in Figure 5. The plot shows that the degree of quenching depends on the structure of the alcohol.

The magnitude of the quenching can be quantified as log (I_o/I) where I_o is the fluorescence intensity in a reference solvent (toluene) and I is the fluorescence intensity in the sample solvent. A plot of the quenching magnitude vs. Catalán's solvent acidity parameter (SA) is shown in Figure 6. The SA parameter is a measure of the H-bond donating ability of the solvent [32]. The plot indicates that the degree of quenching is correlated with the SA parameter. The range of quenching in absolute terms is ~1.5 orders of magnitude going from 2-octanol to methanol. The point for 1-octanol is excluded as it falls anomalously below the line of best fit.

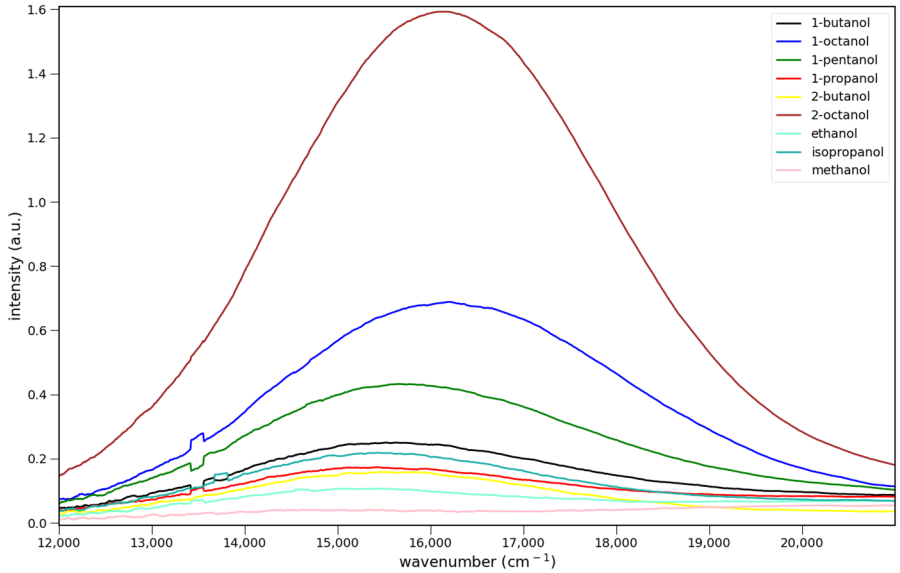

Figure 5. Fluorescence spectra of 1.3×10^{-5} M **6** in protic solvents. Excitation at 365 nm.

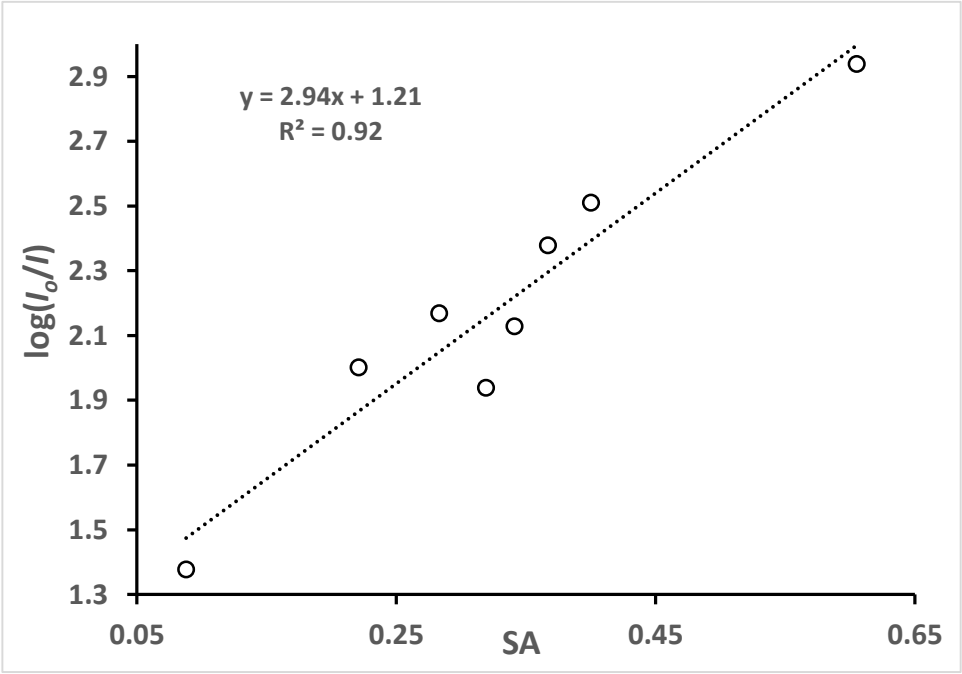

Figure 6. Plot of log (I_o/I) vs. Catalan's solvent acidity parameter (SA) for **6** in the alcohols shown in Figure 5. The point for 1-octanol is excluded.

3.3. Synthesis of 1,5-Acrylodan-Human Serum Albumin Conjugate and Denaturation Studies

3.3.1. Synthesis of AC-HSA

The generation of the 1,5-Acrylodan conjugate with HSA follows the procedure with 2,6-Acrylodan. In both cases, the covalent attachment to the protein is through a Michael reaction with cysteine-34 of HSA. The purification of the conjugate is performed using dialysis size-exclusion chromatography to remove the unreacted Acrylodan. The final concentration of the protein conjugate (AC-HSA) is estimated by its absorption at 308 nm. The absorption and emission spectra of AC-HSA are shown in Figure 7.

Confirmation of covalent attachment was determined through extraction experiments. A 50 µM solution of AC-HSA was mixed carefully with an equal volume of toluene. The fluorescence of the extracted aqueous layer at 560 nm was 64% of the original value, while

the toluene layer was only 2%. A 50 µM solution of HSA spiked with 1,5-Prodan and equilibrated for a day showed only 15% residual fluorescence after extraction, while the toluene layer showed 190%.

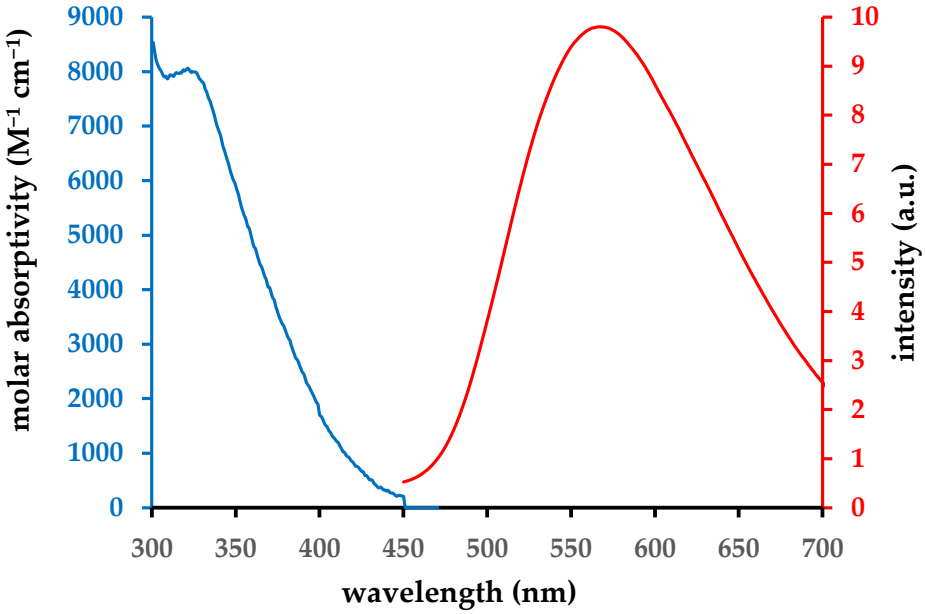

Figure 7. Absorption (**left**, blue) and emission (**right**, red) spectra of 10 µM AC-HSA in phosphate buffer.

3.3.2. Denaturation Studies

Two denaturation experiments were conducted to examine the ability of the Acrylodan moiety as a sensor. In the first, AC-HSA is unfolded with guanidinium hydrochloride (GdmCl) in concentrations approaching 10 M. A plot showing the effect of ion concentration on both the emission intensity and emission maxima is shown in Figure 8. Both the intensity and emission maxima plots are nearly identical. While the intensity varies by a factor of five (0.2 to 1.0), the range of emission maxima is only 600 cm^{-1} (573 to 593 nm). There is an initial increase in intensity and peak position (in cm^{-1}) followed by a steeper decline until bottoming out at the maximum ion concentration.

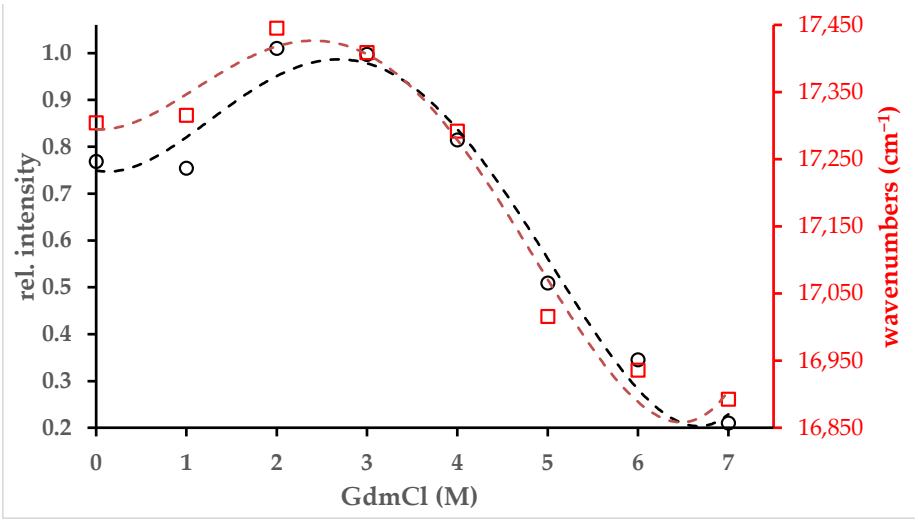

Figure 8. Plots of fluorescence intensity (left vertical axis, black, o) and fluorescence center of gravity (right vertical axis, red, □) vs. guanidinium hydrochloride concentration for 10 µM AC-HSA. Excitation was at 365 nm.

Surfactants are also effective means to unfold proteins. The AC-HSA conjugate was treated with sodium dodecyl sulfate. The amount of SDS varied between zero and ten equivalents. The plots of fluorescence intensity and emission maxima are shown in Figure 9. As with guanidinium hydrochloride, the two plots are very similar. They show a shallow shoulder at the start of the titration followed by a steep decline. The plots reach a minimum near 7 or 8 equivalents of SDS and then start to rise.

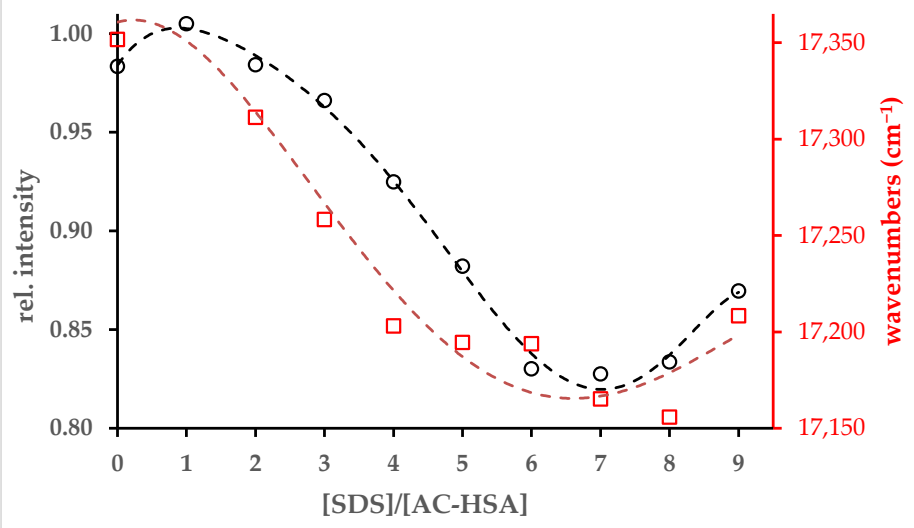

Figure 9. Plots of fluorescence intensity (left vertical axis, black, o) and fluorescence center of gravity (right vertical axis, red, □) vs. SDA equivalents for 10 μM AC-HSA. Excitation was at 365 nm.

4. Discussion

4.1. 1,5-Acrylodan

Despite its simple structure, the preparation of 1,5-Acrylodan proved challenging. The major impediments were the low reactivity of carbonyl derivatives at the 5 position and the tendency for the 5-litho-1-dimethylaminonaphthalene **7** (Figure 10) to abstract a hydrogen atom. We first attempted to prepare **6** using the same route we developed for 2,6-Acrylodan [33]. In this pathway, aryl lithium **7** is treated with acyl pyrrole **8**. Instead of reacting with the carbonyl group, the reaction gave mostly H-atom abstraction, likely from the carbonyl α-hydrogens. Given this propensity for hydrogen abstraction, we treated **7** with carbonyl dipyrrole, an electrophile possessing no α-hydrogens. This reaction gave compound **9** in 74% yield. Aryl acyl pyrroles have been used to generate ketones through DBU-catalyzed decomposition of the intermediate carbinol from a nucleophilic addition [34]. Compound **9** reacted poorly with vinyl magnesium chloride and gave at most a 5% yield of the carbinol. Even more disappointing, the carbinol resisted decomposition with DBU. Compound **9** did react with n-BuLi to give the butyl ketone directly in 76% yield. The successful route treats **7** with ethyl chloroformate, which is also an electrophile without α-hydrogens. Before settling on the Kulinkovich reaction, we tried saponifying ester **3** and converting it to the acid chloride **10**. Even forcing conditions gave only a 14% conversion. The acid chloride reacted moderately well with vinyl magnesium chloride (38%) to give **6** directly without double addition.

While the Kalinkovich reaction gives only a 41% yield, it has the advantage of reacting directly with the ethyl ester, thus reducing the number of steps, and it avoids the issue of double addition. As mentioned, this reaction produces significant byproducts. In practice, the subsequent oxidation with $Cu(OAc)_2$ is carried out on the crude reaction mixture. The Acrylodan is purified by silica gel chromatography. The separation is delicate in that 1,5-Prodan, the saturated version of **6**, results as a byproduct in the last step, and has a similar R_f as **6**.

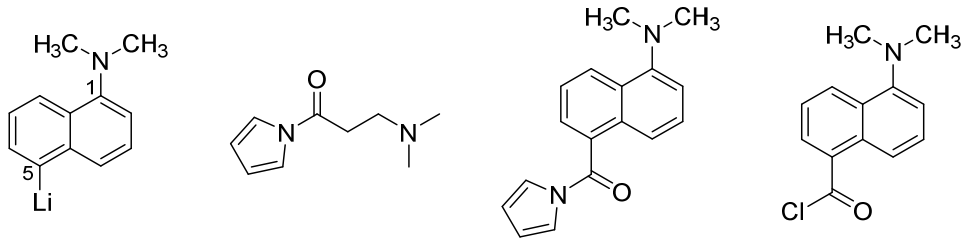

7 **8** **9** **10**

Figure 10. Intermediates in abandoned routes into 1,5-Acrylodan.

The photophysical characteristics of **6** are very similar to 1,5-Prodan (Table 1) [11]. Both have a long wavelength absorption greater than 300 nm. The absorption maximum for **6** is higher energy than 1,5-Prodan. The emission of both varies over a wide range (2100 cm^{-1} vs. 2700 cm^{-1}, respectively) as the solvent polarity increases. 1,5-Prodan responds more strongly to the change in polarity as shown by the slope of $\lambda_{em}{}^{-1}$ vs. $E_T(30)$. Both are strongly fluorescent in toluene but are quenched with protic solvents. The quenching is stronger with 1,5-Acrylodan as shown by both the quantum yield in isopropanol (0.002 vs. 0.021), a solvent with a relatively low SA parameter, and by the slope of the $\log(I_o/I)$ vs. SA quenching plot (2.94 vs. 2.48).

Table 1. Comparison of the photophysical characteristics of 1,5-Acrylodan and 1,5-Prodan.

	λ_{abs} (EtOH) nm	λ_{em} (Tol) nm	λ_{em} (iPrOH) nm	Slope $\lambda_{em}{}^{-1}$ vs. $E_T(30)$	Φ (tol)	Φ (iPrOH)	Slope $\log(I_o/I)$ vs. SA
1,5-Acrylodan	308	573	651	−137	0.26	0.002	2.94
1,5-Prodan	332	544	636	−169	0.44	0.021	2.48

4.2. 1,5-AC-HSA

The acryloyl moiety in **6** and in 2,6-Acrylodan are Michael acceptors. Thiols, in particular, undergo facile Michael addition with the acryloyl group. Compound **6** becomes covalently attached to HSA under mild conditions. Proof of covalent attachment comes from simple extraction studies. By analogy with 2,6-Acrylodan, we assume that attachment occurs at the free thiol of Cys-34. It is possible that attachment occurs at another nucleophilic atom, for example, the nitrogen of Lys-240 near the bilirubin binding site [35,36]. However, this site has a much lower affinity than Cys-34 of HSA for reaction with 2,6-Acrylodan.

A comparison of the protein unfolding experiments shows that the 1,5-Acrylodan conjugate offers more sensitivity to exposure to water. With GdmCl denaturation, 1,5-AC-HSA shows a 25% increase in fluorescence intensity between 0 and 2 M GdmCl, while 2,6-AC-HSA experiences a 15% increase. At these concentrations, Domain II suffers the greater share of unfolding, leaving Domain I and the attached Acrylodan shielded from water incursion. At high GdmCl concentrations (6–7 M), 1,5-AC-HSA loses ~75% of its maximum intensity, while the 2,6-AC-HSA loses ~50% of its fluorescence [28]. On the other hand, the emission maxima with the 1,5-system are less sensitive to water. With GdmCl, emissions vary over 600 cm^{-1} for 1,5-AC-HSA, whereas for 2,6-AC-HSA, the range is 1500 cm^{-1} [28]. While the range is smaller for the 1,5-system, the change in the emission position closely follows that of the fluorescence intensity. Unfolding using SDS shows a much smaller change in fluorescence intensity. The octadecyl chains limit the exposure of the chromophore to water. Nevertheless, the emission intensity and position closely track each other, showing that the sensing mechanism is operating.

5. Conclusions

The preparation of 1,5-Acrylodan has been accomplished in six steps and 19% overall yield. Its fluorescence is sensitive to both the polarity and the H-bonding ability of solvents.

Its utility as a thiol-selective, bioconjugate sensor has been demonstrated with HSA as a model system. Protein unfolding experiments show that the intensity of the fluorescent tag is very sensitive to exposure to water, much more so than the related 2,6-AC-HSA conjugate. On the other hand, the emission position is less sensitive to changes in the micropolarity than the 2,6-AC-HSA conjugate.

Supplementary Materials: The following supporting information can be downloaded at https://www.mdpi.com/article/10.3390/org5040026/s1, ^{1}H and ^{13}CNMR spectra of **4**, **5**, and **6** in $CDCl_3$.

Author Contributions: Conceptualization, C.A.; methodology, J.M. and C.A.; formal analysis, C.A., J.M. and M.P.; investigation, J.M., M.P. and C.A.; data curation, J.M., C.A. and M.P.; writing—original draft preparation, J.M.; writing—review and editing, C.A. and J.M.; supervision, C.A. All authors have read and agreed to the published version of the manuscript.

Funding: This research received no external funding.

Data Availability Statement: The data presented in this study are available either in this article or in the Supplementary Materials.

Conflicts of Interest: The authors declare no conflicts of interest.

References

1. Padeste, C.; Grubelnik, A.; Tiefenauer, L. Ferrocene–Avidin Conjugates for Bioelectrochemical Applications. *Biosens. Bioelectron.* **2000**, *15*, 431–438. [CrossRef] [PubMed]
2. Sahoo, H. Fluorescent Labeling Techniques in Biomolecules: A Flashback. *RSC Adv.* **2012**, *2*, 7017. [CrossRef]
3. Hermanson, G.T. *Bioconjugate Techniques*, 2nd ed.; Elsevier Science: Burlington, MA, USA, 2010; ISBN 978-0-12-370501-3.
4. Fanali, G.; Di Masi, A.; Trezza, V.; Marino, M.; Fasano, M.; Ascenzi, P. Human Serum Albumin: From Bench to Bedside. *Mol. Asp. Med.* **2012**, *33*, 209–290. [CrossRef]
5. Wysocki, L.M.; Lavis, L.D. Advances in the Chemistry of Small Molecule Fluorescent Probes. *COCHBI* **2011**, *15*, 752–759. [CrossRef] [PubMed]
6. Parisio, G.; Marini, A.; Biancardi, A.; Ferrarini, A.; Mennucci, B. Polarity Sensitive Fluorescent Probes in Lipid Bilayers: Bridging Spectroscopic Behavior and Microenvironment Properties. *J. Phys. Chem. B* **2011**, *115*, 9980–9989. [CrossRef]
7. Chapman, C.F.; Maroncelli, M. Fluorescence Studies of Solvation and Solvation Dynamics in Ionic Solutions. *J. Phys. Chem.* **1991**, *95*, 9095–9114. [CrossRef]
8. Niko, Y.; Kawauchi, S.; Konishi, G. Solvatochromic Pyrene Analogues of Prodan Exhibiting Extremely High Fluorescence Quantum Yields in Apolar and Polar Solvents. *Chem. Eur. J.* **2013**, *19*, 9760–9765. [CrossRef]
9. Thakur, R.; Das, A.; Chakraborty, A. Interaction of Human Serum Albumin with Liposomes of Saturated and Unsaturated Lipids with Different Phase Transition Temperatures: A Spectroscopic Investigation by Membrane Probe PRODAN. *RSC Adv.* **2014**, *4*, 14335–14347. [CrossRef]
10. Krishnakumar, S.S.; Panda, D. Spatial Relationship between the Prodan Site, Trp-214, and Cys-34 Residues in Human Serum Albumin and Loss of Structure through Incremental Unfolding. *Biochemistry* **2002**, *41*, 7443–7452. [CrossRef]
11. Chen, T.; Lee, S.W.; Abelt, C.J. 1,5-Prodan Emits from a Planar Intramolecular Charge-Transfer Excited State. *ACS Omega* **2018**, *3*, 4816–4823. [CrossRef]
12. Zharkova, O.M.; Rakhimov, S.I.; Morozova, Y.P. Quantum-Chemical Investigation of the Spectral Properties of Fluorescent Probes Based on Naphthalene Derivatives (Prodan, Promen). *Russ. Phys. J.* **2013**, *56*, 411–419. [CrossRef]
13. Nikitina, Y.Y.; Iqbal, E.S.; Yoon, H.J.; Abelt, C.J. Preferential Solvation in Carbonyl-Twisted PRODAN Derivatives. *J. Phys. Chem. A* **2013**, *117*, 9189–9195. [CrossRef] [PubMed]
14. Prendergast, F.G.; Meyer, M.; Carlson, G.L.; Iida, S.; Potter, J.D. Synthesis, Spectral Properties, and Use of 6-Acryloyl-2-Dimethylaminonaphthalene (Acrylodan). A Thiol-Selective, Polarity-Sensitive Fluorescent Probe. *J. Biol. Chem.* **1983**, *258*, 7541–7544. [CrossRef] [PubMed]
15. Kawski, A. Ground-and Excited-State Dipole Moments of 6-Propionyl-2-(Dimethylamino) Naphthalene Determined from Solvatochromic Shifts. *Zeit. Naturforsch. A* **1999**, *54*, 379–381. [CrossRef]
16. Chalovich, J.M.; Lutz, E.; Baxley, T.; Schroeter, M.M. Acrylodan-Labeled Smooth Muscle Tropomyosin Reports Differences in the Effects of Troponin and Caldesmon in the Transition from the Active State to the Inactive State. *Biochemistry* **2011**, *50*, 6093–6101. [CrossRef]
17. Hickey, J.M.; Sahni, N.; Chaudhuri, R.; D'Souza, A.; Metters, A.; Joshi, S.B.; Russell Middaugh, C.; Volkin, D.B. Effect of Acrylodan Conjugation and Forced Oxidation on the Structural Integrity, Conformational Stability, and Binding Activity of a Glucose Binding Protein SM4 Used in a Prototype Continuous Glucose Monitor. *Prot. Sci.* **2017**, *26*, 527–535. [CrossRef]
18. Allert, M.J.; Hellinga, H.W. Discovery of Thermostable, Fluorescently Responsive Glucose Biosensors by Structure-Assisted Function Extrapolation. *Biochemistry* **2022**, *61*, 276–293. [CrossRef]

19. Hibbs, R.E.; Talley, T.T.; Taylor, P. Acrylodan-Conjugated Cysteine Side Chains Reveal Conformational State and Ligand Site Locations of the Acetylcholine-Binding Protein. *J. Biol. Chem.* **2004**, *279*, 28483–28491. [CrossRef]
20. Fruen, B.R.; Balog, E.M.; Schafer, J.; Nitu, F.R.; Thomas, D.D.; Cornea, R.L. Direct Detection of Calmodulin Tuning by Ryanodine Receptor Channel Targets Using a Ca 2+ -Sensitive Acrylodan-Labeled Calmodulin. *Biochemistry* **2005**, *44*, 278–284. [CrossRef]
21. Simard, J.R.; Kamp, F.; Hamilton, J.A. Acrylodan-Labeled Intestinal Fatty Acid-Binding Protein to Measure Concentrations of Unbound Fatty Acids. In *Methods in Membrane Lipids*; Dopico, A.M., Ed.; Methods in Molecular Biology; Humana Press: Totowa, NJ, USA, 2007; Volume 400, pp. 27–43. ISBN 978-1-58829-662-7.
22. Lutz, E.; Schroeter, M.M.; Baxley, T.; Chalovich, J.M. Kinetics of Smooth Muscle Acrylodan-Tropomyosin Transitions on Actin. *Biophys. J.* **2011**, *100*, 113a–114a. [CrossRef]
23. Kivi, R.; Loog, M.; Jemth, P.; Järv, J. Kinetics of Acrylodan-Labelled cAMP-Dependent Protein Kinase Catalytic Subunit Denaturation. *Protein J.* **2013**, *32*, 519–525. [CrossRef] [PubMed]
24. Flora, K.; Brennan, J.D.; Baker, G.A.; Doody, M.A.; Bright, F.V. Unfolding of Acrylodan-Labeled Human Serum Albumin Probed by Steady-State and Time-Resolved Fluorescence Methods. *Biophys. J.* **1998**, *75*, 1084–1096. [CrossRef] [PubMed]
25. Tayyab, S.; Siddiqui, M.U.; Ahmad, N. Experimental Determination of the Free Energy of Unfolding of Proteins. *Biochem. Ed.* **1995**, *23*, 162–164. [CrossRef]
26. Lakowicz, J.R. *Principles of Fluorescence Spectroscopy*; Springer US: Boston, MA, USA, 1999; ISBN 978-1-4757-3063-0.
27. Wang, R.; Sun, S.; Bekos, E.J.; Bright, F.V. Dynamics Surrounding Cys-34 in Native, Chemically Denatured, and Silica-Adsorbed Bovine Serum Albumin. *Anal. Chem.* **1995**, *67*, 149–159. [CrossRef]
28. Kamal, J.K.; Zhao, L.; Zewail, A.H. Ultrafast Hydration Dynamics in Protein Unfolding: Human Serum Albumin. *Proc. Natl. Acad. Sci. USA* **2004**, *101*, 13411–13416. [CrossRef]
29. Horner, L.; Hallenbach, W.; Vogt, M. Chemie an Starren Grenzflächen, 11. Aerosile Mit Kovalent Beweglich Und Starr Verknüpften Fluoreszenzträgern / Chemistry on Rigid Surfaces, 11. Aerosils with Covalently Movable and Rigid Linked Fluorophors. *Zeit. Naturforsch. B* **1989**, *44*, 225–232. [CrossRef]
30. Kulinkovich, O.G.; Sviridov, S.V.; Vasilevski, D.A. Titanium(IV) Isopropoxide-Catalyzed Formation of 1-Substituted Cyclopropanols in the Reaction of Ethylmagnesium Bromide with Methyl Alkanecarboxylates. *Synthesis* **1991**, *1991*, 234. [CrossRef]
31. Reichardt, C.; Welton, T. *Solvents and Solvent Effects in Organic Chemistry*; Wiley-VCH Verlag GmbH: Weinheim, Germany, 2011.
32. Catalán, J.; Díaz, C. A Generalized Solvent Acidity Scale: The Solvatochromism of *o-tert*-Butylstilbazolium Betaine Dye and Its Homomorph o, o′-Di-tert-butylstilbazolium Betaine Dye. *Liebigs Ann. Chem.* **1997**, *1997*, 1941–1949. [CrossRef]
33. Silvonek, S.S.; Giller, C.B.; Abelt, C.J. Alternate Syntheses of Prodan and Acrylodan. *Org. Prep. Proced. Int.* **2005**, *37*, 589–594. [CrossRef]
34. Evans, D.A.; Borg, G.; Scheidt, K.A. Remarkably Stable Tetrahedral Intermediates: Carbinols from Nucleophilic Additions to *N*-Acylpyrroles. *Angew. Chem. Int. Ed.* **2002**, *41*, 3188–3191. [CrossRef]
35. Moreno, F.; Cortijo, M.; González-Jiménez, J. Interaction of Acrylodan with Human Serum Albumin. A Fluorescence Spectroscopic Study. *Photochem. Photobiol.* **1999**, *70*, 695–700. [CrossRef]
36. Petersen, C.E.; Ha, C.-E.; Harohalli, K.; Feix, J.B.; Bhagavan, N.V. A Dynamic Model for Bilirubin Binding to Human Serum Albumin. *J. Biol. Chem.* **2000**, *275*, 20985–20995. [CrossRef]